

# Mechanical efficiency and reflux of peristaltic pumping through a finite length vessel

D. Tripathi, S. K. Pandey and M. K. Chaube

*Department of Applied Mathematics,  
Institute of Technology, Banaras Hindu University, Varanasi-221005, INDIA  
Email: [dtripathi.rs.apm@itbhu.ac.in](mailto:dtripathi.rs.apm@itbhu.ac.in)*

## Abstract:

This paper is aimed at studying mechanical efficiency and reflux of unsteady peristaltic pumping through finite length vessels. Expressions for the axial and transverse velocities have been derived for creeping flow. The wall equations of vessels have been so assumed that they can find application for flows in oesophagus and in pumps with similar wall vibrations. The pressure distribution and local wall shear stress for free pumping have been studied in the laboratory frame of reference. It is observed during temporal examination that pressure and local wall shear stress distributions for channel and tubular flows are qualitatively similar but quantitatively quite different. Mechanical efficiency of peristaltic pump for tubular flow is larger than channel flow. Tubular flow is more prone to the occurrence of reflux.

**Keywords:** Peristalsis; Oesophagus; Newtonian fluid; Mechanical efficiency; Reflux.

## 1 Introduction

Peristaltic transport is the transportation of physiological fluids by peristalsis, which is defined as a series of coordinated continuous rhythmic muscle contraction followed by relaxation. It is also defined as the pumping without piston. The flow of blood through arteries and veins, the flow of urine through ureter, the flow of bile from gall bladder into duodenum, the movement of chyme in entire gastro intestinal tract, transportation of food bolus through alimentary canal and the movement of some worms are some examples of peristaltic transport. Peristaltic pumps work in accordance with this mechanism as mechanical pumps, without maligning the purity of the fluid contained.

The two aspects we choose to discuss here are mechanical efficiency and reflux which have been bearing importance for scientific investigation right from their initial estimation for Newtonian fluid in an infinite tube by Shapiro et al. [1]. Mechanical efficiency is a physical property of peristaltic pump, which is defined as the ratio between the average rate per wavelength at which work is done by the moving fluid against a pressure head and average at which the walls do work on the fluid, while reflux is a phenomenon, which refers to the presence of fluid particles that move, on the average, in a direction opposite to the net flow (cf. Shapiro et al. [1]). Backward migration of bacteria against the direction of the urine flows and gastro-oesophageal reflux (cf. Keri Dorst [2]) are a few examples of reflux.

Shapiro et al. [1] reported that the mechanical efficiency, as defined above, is less for axisymmetric case than that in the channel case. Takabatake et al. [3, 4] who applied finite difference technique to solve the problem of peristaltic pumping made a comparative study of reflux and mechanical efficiency in channel and axisymmetric tube, pointed out a mistake in the calculation and concluded that the efficiency in the tubular configuration is much higher than that in the two-dimensional plane configuration for all values of the amplitude of wall vibrations. They further concluded that peristaltic reflux is much stronger for tube than for channel. Brasseur et al. [5]

estimated the same for a two-layered Newtonian fluid for the channel flow; and they reported that pumping is degraded by the presence of a lesser viscous peripheral layer. A subsequent revelation for the same problem for axisymmetric case was reported by Rao and Usha [6]. In another paper, they [7] discussed the mechanical efficiency of peristaltic flows in an elliptic cross section for varying amplitudes. Misra and Pandey [8, 9] made a comparative study of mechanical efficiency for different values of viscosity, amplitude and fluid behavior index. They inferred that mechanical efficiency increases with the increasing values of amplitude, viscosity and fluid behavior index. They also discussed the reflux phenomenon for power law fluids with a peripheral layer. Eytan et al. [10] have studied reflux theoretically for peristaltic transport in a tapered channel.

More recently Elshehawey and Gharseldien [11] studied the effects of the variation of the viscosities on the mechanical efficiency and they also found that the mechanical efficiency increases with increasing viscosity. Rao and Mishra [12, 13] have also studied reflux phenomenon for different values of fluid behavior index, Darcy number and viscosity.

If investigation is from application point of view, for example, for oesophagus which is not very large, we opine that analysis should be for finite lengths and also for inward unidirectional vibrations. None of those analyses are based on finite length tubes and for the wave propagation that lets walls vibrate inwards only. Keeping these points in mind we carry out a two-dimensional analysis for a Newtonian fluid in a finite length channel, from which pumping efficiency is estimated.

Li and Brasseur [14] derived expressions of the pressure distribution and local wall shear stress for the axisymmetric case of a finite length tube, but they did not discuss the mechanical efficiency and reflux for that case. Therefore, the additional results of pumping efficiency and reflux for the tubular flow are derived from their analyses. However, the wall equations are different form what they assumed. We follow the one suggested by Misra and Pandey [15] for both the geometries.

## 2 Analysis for channel flow

The governing equations are given by

$$\left. \begin{aligned} \rho \left( \frac{\partial}{\partial t} + \tilde{u} \frac{\partial}{\partial \xi} + \tilde{v} \frac{\partial}{\partial \eta} \right) \tilde{u} &= -\frac{\partial \tilde{p}}{\partial \xi} + \mu \left( \frac{\partial^2 \tilde{u}}{\partial \xi^2} + \frac{\partial^2 \tilde{u}}{\partial \eta^2} \right), \\ \rho \left( \frac{\partial}{\partial t} + \tilde{u} \frac{\partial}{\partial \xi} + \tilde{v} \frac{\partial}{\partial \eta} \right) \tilde{v} &= -\frac{\partial \tilde{p}}{\partial \eta} + \mu \left( \frac{\partial^2 \tilde{v}}{\partial \xi^2} + \frac{\partial^2 \tilde{v}}{\partial \eta^2} \right), \\ \frac{\partial \tilde{u}}{\partial \xi} + \frac{\partial \tilde{v}}{\partial \eta} &= 0, \end{aligned} \right\} \quad (2.1)$$

where  $\rho, \mu, \tilde{\xi}, \tilde{\eta}, \tilde{t}, \tilde{u}, \tilde{v}, \tilde{p}$  symbolise respectively fluid density, viscosity, axial coordinate, transverse coordinate, time, axial velocity, transverse velocity, and pressure.

We assume that the vibrations of the walls are caused by the propagation of progressive contraction waves given by (cf. Misra and Pandey [15])

$$\tilde{h}(\tilde{\xi}, \tilde{t}) = a - \tilde{\phi} \cos^2 \frac{\pi}{\lambda} (\tilde{\xi} - c\tilde{t}). \quad (2.2)$$

Then we introduce the following non-dimensional parameters;

$$\left. \begin{aligned} \xi &= \frac{\tilde{\xi}}{\lambda}, \quad \eta = \frac{\tilde{\eta}}{a}, \quad t = \frac{c\tilde{t}}{\lambda}, \quad u = \frac{\tilde{u}}{c}, \quad v = \frac{\tilde{v}}{c\alpha}, \quad h = \frac{\tilde{h}}{a}, \quad l = \frac{\tilde{l}}{\lambda}, \\ \phi &= \frac{\tilde{\phi}}{a}, \quad p = \frac{\tilde{p}a^2}{\mu c\lambda}, \quad \psi = \frac{\tilde{\psi}}{ac}, \quad Q = \frac{\tilde{Q}}{ac}, \quad Re = \rho ca/\mu, \end{aligned} \right\} \quad (2.3)$$

where  $c, \lambda, a, \alpha$  are respectively wave velocity, wavelength, half width of the channel and wave number defined as  $\alpha = \frac{a}{\lambda}$ ;  $\tilde{h}, \tilde{\phi}, \tilde{\psi}, \tilde{Q}$  represent respectively transverse vibration of the walls, amplitude of the wave, stream function and volume flow rate while  $\xi, \eta, t, u, v, h, l, \phi, p, \psi, Q$  stand respectively for dimensionless counterparts of the dimensional parameters.

Further, applying long wavelength approximations and neglecting convective acceleration terms in comparison to viscous terms for small Reynolds number  $Re$ , the governing Eqs. 2.1, in view of the

above non-dimensionalisation, reduce to

$$\left. \begin{aligned} \frac{\partial p}{\partial \xi} &= \frac{\partial^2 u}{\partial \eta^2}, \quad \frac{\partial p}{\partial \eta} = 0, \\ \frac{\partial u}{\partial \xi} + \frac{\partial v}{\partial \eta} &= 0. \end{aligned} \right\} \quad (2.4)$$

We then impose the following boundary conditions on the governing equations;

$$u(\xi, h, t) = 0, v(\xi, h, t) = \frac{\partial h}{\partial t}, \frac{\partial u(\xi, 0, t)}{\partial \eta} = 0, v(\xi, 0, t) = 0 \quad (2.5)$$

The axial and the transverse velocities are obtained from Eq.2.4 using Eq.2.5 as

$$u = \frac{1}{2} \frac{\partial p}{\partial \xi} (\eta^2 - h^2), \quad (2.6)$$

$$v = \frac{\eta}{6} \left\{ 6h \frac{\partial h}{\partial \xi} \frac{\partial p}{\partial \xi} - \frac{\partial^2 p}{\partial \xi^2} (\eta^2 - 3h^2) \right\}. \quad (2.7)$$

Moreover, the pressure gradient is also determined from Eq.2.7 and the second boundary condition of 2.5 as

$$\frac{\partial p}{\partial \xi} = \frac{1}{h^3} \left[ \gamma(t) + 3 \int_0^\xi \frac{\partial h}{\partial t} ds \right], \quad (2.8)$$

where  $\gamma(t)$  is the integrating constant, which will be evaluated later.

Integrating from 0 to  $\xi$ , Eq.2.8 yields

$$p(\xi, t) - p(0, t) = \int_0^\xi \frac{1}{h^3} \left\{ \gamma(t) + 3 \int_0^s \frac{\partial h}{\partial t} ds_1 \right\} ds. \quad (2.9)$$

Substituting  $\xi = l$  in Eq.2.9, the pressure across the two ends of the finite channel is given by

$$\Delta p_l(t) = p(l, t) - p(0, t) = \int_0^l \frac{1}{h^3} \left\{ \gamma(t) + 3 \int_0^s \frac{\partial h}{\partial t} ds_1 \right\} ds, \quad (2.10)$$

which gives  $\gamma(t)$  as

$$\gamma(t) = \frac{\Delta p_l(t) - 3 \int_0^l \frac{1}{h^3} \int_0^\xi \frac{\partial h}{\partial t} ds}{\int_0^l h^{-3} d\xi}. \quad (2.11)$$

The local wall shear stress is derived as

$$\tau_w(\xi, t) = \left. \frac{\partial u}{\partial \eta} \right|_{\eta=h} = \frac{1}{h^2} \left[ \gamma(t) + 3 \int_0^\xi \frac{\partial h}{\partial t} ds \right]. \quad (2.12)$$

### 2.1 Analysis for volume flow rate

The non-dimensional volume flow rate is given by

$$Q(\xi, t) = \beta \frac{\tilde{Q}(\tilde{\xi}, \tilde{t})}{ac} = -\frac{\beta}{3} \frac{\partial p}{\partial \xi} h^3, \quad (2.13)$$

where  $\beta = 1$  for train wave and  $\beta = l/\lambda$  for single wave transport.

The averaged flow rate in the laboratory frame is obtained by averaging Eq.2.13 for one time period, which is given by

$$\bar{Q} = \int_0^1 Q dt = - \int_0^1 \frac{\beta}{3} \frac{\partial p}{\partial \xi} h^3 dt. \quad (2.14)$$

Using Eq.2.8 into Eq.2.13, the flow rate is expressed in terms of inlet flow rate as

$$Q(\xi, t) = Q(0, t) - \frac{\beta}{3} \int_0^\xi \frac{\partial h}{\partial t} ds, \quad (2.15)$$

The relation between the flow rate and the pressure difference is obtained, by integrating Eq.2.13 after certain manipulations, as

$$p(\xi, t) - p(0, t) = -\frac{\beta}{3} \int_0^\xi \frac{Q(s, t)}{h^3} ds. \quad (2.16)$$

For  $\xi = l$ , Eq.2.16 gives the pressure difference  $\Delta p_l(t)$  in between the inlet and the outlet of the channel in the form

$$\Delta p_l(t) = p(l, t) - p(0, t) = -\frac{\beta}{3} \int_0^l \frac{Q(s, t)}{h^3} ds. \quad (2.17)$$

### 3 Mechanical Efficiency

The mechanical efficiency of a peristaltic pump for channel flow is obtained as

$$E = \frac{\bar{Q} \Delta p_1}{\frac{\phi}{2} \int_0^1 \int_0^1 \frac{\partial p}{\partial \xi} \cos 2\pi(\xi - t) d\xi dt}, \quad (3.1)$$

where  $\Delta p_1$  is the pressure difference across one wavelength and it is expressed as

$$\Delta p_1 = -\frac{3}{\beta} \int_0^1 \left( \frac{\bar{Q} - 1 + \frac{\phi}{2}}{h^3} + \frac{1}{h^2} \right) d\xi. \quad (3.2)$$

Maximum averaged flow rate  $\bar{Q}_0$  is evaluated by substituting  $\Delta p_1 = 0$  in Eq.3.2 and we get

$$\bar{Q}_0 = \left( 1 - \frac{\phi}{2} - \frac{\int_0^1 h^{-2} d\xi}{\int_0^1 h^{-3} d\xi} \right). \quad (3.3)$$

For axisymmetric case, the mechanical efficiency can be derived as

$$E = \frac{\Delta p_1 \bar{Q}}{\frac{3\phi^2}{8} \Delta p_1 + \int_0^1 \int_0^1 \frac{\partial p}{\partial \xi} \{ \phi \cos 2\pi(\xi - t) - \phi^2 \cos^4 \pi(\xi - t) \} d\xi dt}, \quad (3.4)$$

where  $\Delta p_1$  can be easily derived from the analyses given in Li and Brasseur [14] as

$$\Delta p_1 = -\frac{8}{\beta} \int_0^1 \left( \frac{\bar{Q} - 1 + \phi - \frac{3\phi^2}{8}}{h^4} + \frac{1}{h^2} \right) d\xi \quad (3.5)$$

and maximum flow rate is

$$\bar{Q}_0 = \left( 1 - \phi + \frac{3\phi^2}{8} - \frac{\int_0^1 h^{-2} d\xi}{\int_0^1 h^{-4} d\xi} \right). \quad (3.6)$$

## 4 Reflux limit

### 4.1 Channel flow

The dimensional form of the stream function in the wave frame is defined as

$$d\tilde{\psi} = \tilde{U}d\tilde{\zeta} - \tilde{V}d\tilde{\zeta}, \quad (4.1)$$

where  $\tilde{\psi}, \tilde{\zeta}, \tilde{U}$  and  $\tilde{V}$  are stream function, axial and transverse coordinates, axial and transverse velocities respectively. Using the transformations between the wave and the laboratory frames, defined as

$$\tilde{\zeta} = \xi - ct, \tilde{\zeta} = \tilde{\eta}, \tilde{U} = \tilde{u} - c, V = v, \tilde{q} = \tilde{Q} - c\tilde{h}, \tilde{\Psi} = \tilde{\psi} - \tilde{\eta}, \quad (4.2)$$

where the parameters on the left side are in the wave frame and that on the right side are in the laboratory frame, we obtain the stream function as

$$\psi = - \left[ \frac{3}{2} \left( \frac{\bar{Q} - 1 + \frac{\phi}{2} + h}{h^3} \right) \left( \frac{\eta^3}{3} - \eta h^2 \right) + \eta \right]. \quad (4.3)$$

At the wall, we have

$$\psi|_{\eta=h} = \psi_w = \bar{Q} - 1 + \frac{\phi}{2} \quad (4.4)$$

The instantaneous flow rate,  $Q_\psi(\xi)$ , defined as

$$Q_\psi(\xi) = \int_0^\eta u(\xi, \eta, t) d\eta \text{ reduces to } Q_\psi(\xi) = \psi + \eta(\psi, \xi) \quad (4.5)$$

Averaging the above equation for one cycle, it is expressed as

$$\bar{Q}_\psi = \psi + \int_0^1 \eta(\psi, \xi) d\xi \quad (4.6)$$

In order to evaluate the reflux limit,  $\bar{Q}_\psi$  is expanded in power series in terms of a small parameter  $\varepsilon$  about the wall, where  $\varepsilon = \psi - \psi_w$  and it is subjected to the reflux condition

$$\frac{\bar{Q}_\psi}{\bar{Q}_w} > 1 \text{ as } \varepsilon \rightarrow 0 \quad (4.7)$$

The coefficients of the first two terms in the expansion of  $\eta$ , i.e.,

$$\eta = h + a_1\varepsilon + a_2\varepsilon^2 + \dots \quad (4.8)$$

are found by using Eq.4.3, as given below

$$a_1 = -1, \quad a_2 = -\frac{3}{2} \left( \frac{\bar{Q} - 1 + \frac{\phi}{2} + h}{h^2} \right) \quad (4.9)$$

Integrating Eq.4.6, and using Eqs.4.7, 4.8 and 4.9, we obtain the reflux as

$$\bar{Q} < 1 - \frac{\phi}{2} - \frac{\int_0^1 h^{-1} d\xi}{\int_0^1 h^{-2} d\xi}. \quad (4.10)$$

## 4.2 Axisymmetric flow

In order to evaluate the reflux limit, the dimensional form of stream function in the wave frame is defined as

$$d\tilde{\psi} = 2\pi\tilde{R}(\tilde{U}d\tilde{R} - \tilde{V}d\tilde{\zeta}) \quad (4.11)$$

where  $\tilde{R}$ ,  $\tilde{U}$  and  $\tilde{V}$  represent radial coordinate, axial velocity and radial velocity respectively. The transformation between the wave frame and laboratory frame are, in this case, given by

$$\zeta = \xi - t, \quad R = r, \quad U = u - t, \quad V = v, \quad q = Q - h^2, \quad \Psi = \psi - r^2 \quad (4.12)$$

where the left sides of the above equations represent the parameters in wave frame and the right sides represent that in laboratory frame. Using these transformations, the stream function is obtained as

$$\psi = \left( \frac{\bar{Q} - 1 + \phi - \frac{3\phi^2}{8} + h^2}{h^4} \right) (2r^2h^2 - r^2) - r^2 \quad (4.13)$$

At the wall, the stream function is defined as

$$\psi|_{r=h} = \psi_w = \bar{Q} - 1 + \phi - \frac{3\phi^2}{8} \quad (4.14)$$

The instantaneous flow rate is obtained as

$$Q_\psi(\xi) = \psi + r^2(\psi, \xi) \quad (4.15)$$

Averaged over one cycle, this becomes

$$\bar{Q}_\psi = \psi + \int_0^1 r^2(\psi, \xi) d\xi. \quad (4.16)$$

In order to evaluate above integration, using perturbation method,  $r^2(\psi, x)$  is expanded in a power series in terms of a small parameters  $\varepsilon$  about the wall as

$$r^2(\psi, \xi) = h^2 + a_1\varepsilon + a_2\varepsilon^2 + \dots \quad (4.17)$$

In view of Eq.4.17, Eq.4.13 yield

$$a_1 = -1, \quad a_2 = - \left\{ \frac{\bar{Q} - 1 + \phi - \frac{3\phi^2}{8} + h^2}{h^4} \right\} \quad (4.18)$$

The reflux limit is derived as

$$\bar{Q} < 1 - \phi + \frac{3\phi^2}{8} - \frac{\int_0^1 h^{-2} d\xi}{\int_0^1 h^{-4} d\xi}. \quad (4.19)$$

## 5 Numerical results and discussion

In order to investigate the temporal dependence of pressure on the axial distance we plot graphs, for the instant  $t = 0.0, 0.25, 0.5, 0.75, 1.0$ , based on Eq.2.9 in conjunction with Eq.2.11, where  $\Delta p_l(t) = 0$  (i.e., free pumping). We consider train wave propagation (in particular, we consider two waves in the train) on the walls of the channel. The details of the values used for various parameters are given in the captions.

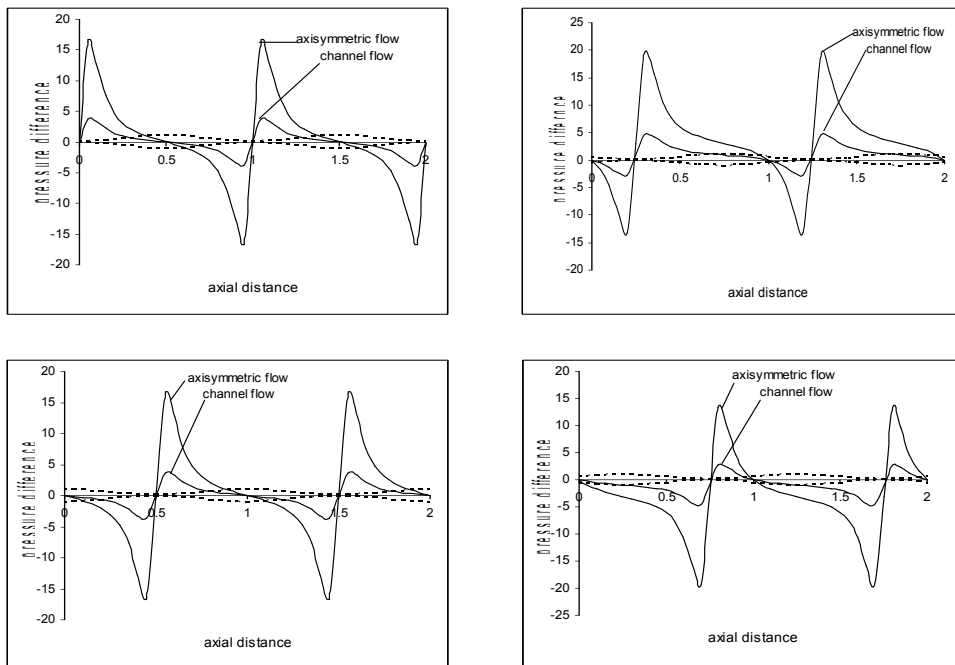


Figure 1: Pressure vs. axial distance at five time instants  $t = 0.0, 0.25, 0.50, 0.75, 1.0$ . Dotted lines (....) represent the position of waves, whereas continuous lines (—) represent the pressure distribution at the amplitude  $\phi = .9$

It is found that once a bolus has already entered into the oesophagus for  $t = 0$  (cf. Fig.1a), the pressure at the inlet is high enough to prevent a backward motion. The pressure is at its maximal peak near the tail of the bolus, and then there is a sharp non-linear decline of pressure to zero at the middle, which further diminishes to its minimal peak. The pressure rises very sharp and linearly, almost vertically, to zero at the head of the bolus and maintains the same trend to reach another maximal peak equal to the previous maximal. This rise of pressure can be attributed to restrain a retrograde motion of the leading bolus in motion. The pressure distribution for the leading bolus is identical. It is observed that the final pressure at the head of the leading bolus is zero as desired. This rise of pressure to zero indicates a controlled motion of bolus which is ready to be delivered to the stomach through the cardiac sphincter which permanently blocks any possible retrograde flow by closing the sphincter. This mechanism of channel flow is found to be qualitatively similar to the tubular flow. The tubular analysis was carried out by Misra and Pandey [15]. However, there is a vast quantitative difference.

For  $t = 0.25$  (cf. Fig.1b), when a portion of a new bolus is in the process of swallowing into the oesophagus and one fourth of the leading bolus has already been inserted into the stomach, the pressure distribution at the inlet appears declining to give way to the incoming bolus and falling of pressure from the peak to zero at the outlet gives a gesture favorable to the movement into the stomach.

For  $t = 0.5$  and  $t = 0.75$ , revealed by Figs.(1c) and (1d) respectively, the pressure distributions depict a continuous process of bolus movement from the mouth to the stomach. When  $t = 1.0$ , the pressure distribution is identical with the one for  $t = 0$ , which indicates that the pumping organ is ready with a new set of bolus as the previous ones have already been delivered to the stomach. The same revelations are predicted for a peristaltic pump of finite size.

It is further observed that the pressure distribution for similar wall equations (cf. Li and Brasseur [14]) but designed in a different way show a similar trend. However, the nature of rising

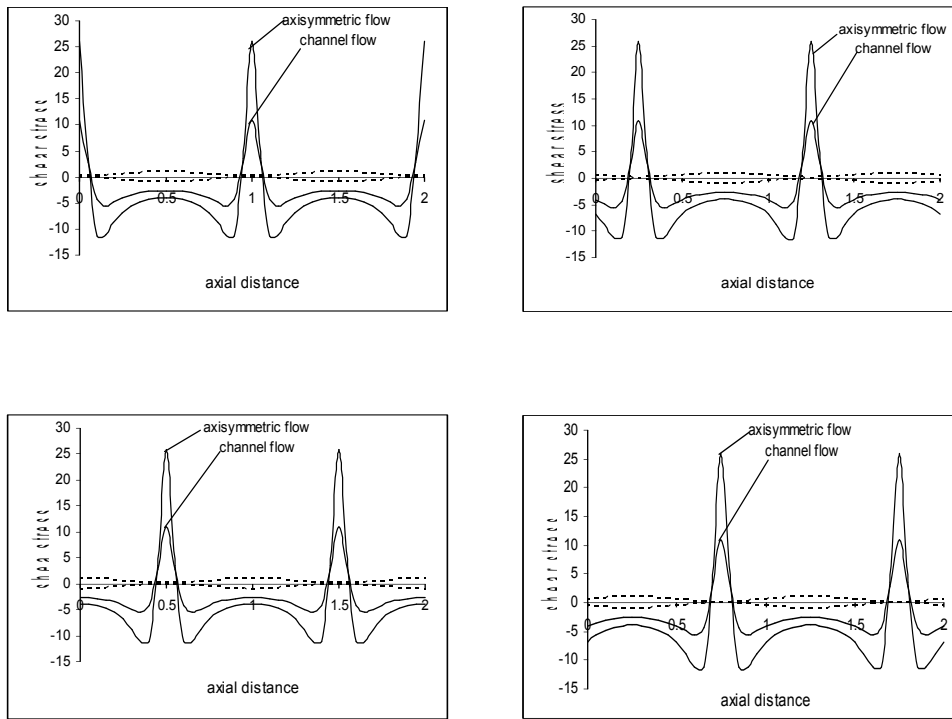


Figure 2: Local wall shear stress vs. axial distance along the finite length vessels at five time instants. Dotted lines (...) represent the position of the wave, whereas the continuous lines (—) represent shear stress distributions for the channel flow and axisymmetric flow at  $\phi = .9$ .

and dropping of pressure along the axial distance experience some dissimilarity.

Moreover, when we plot graphs for temporal examination of axial distance versus local wall shear stress, it is observed that the channel and axisymmetric flows are qualitatively similar as expected but quantitative difference is quite significant (Fig. 2). Figures are self-explanatory.

A plot between averaged flow rate and pressure difference for a particular value of amplitude shows an expected linear relationship. Increasing pressure difference restrains the flow in both the channel and tubular cases. Besides, it is observed that the flow rate for a given pressure difference will be much more in axisymmetric case compared with channel case (cf. Fig. 3).

## 5.1 Application to bolus transport in oesophagus

Water is a well known Newtonian fluid. Here we intend to study the movement of such a fluid in the oesophagus with contraction and relaxation of its walls. Since the shape of the oesophagus hardly remains uniformly circular during propellation of fluid, nor there is any significant intra-circulation, we may consider the flow as two-dimensional. It is possible to have more than one bolus of water in the oesophagus at a time.

## 5.2 Mechanical Efficiency

A graph is plotted for  $\bar{Q}/\bar{Q}_0$  vs.  $E$ , i.e., the ratio of averaged flow rate and maximum flow rate vs. the pumping efficiency, to study the effects of the amplitude on pumping efficiency. It is observed that efficiency increases with amplitude and  $E$  increases with  $\bar{Q}/\bar{Q}_0$ . It is further observed that the pumping efficiency for channel case is less than that for the axisymmetric case (cf. Fig. 4).



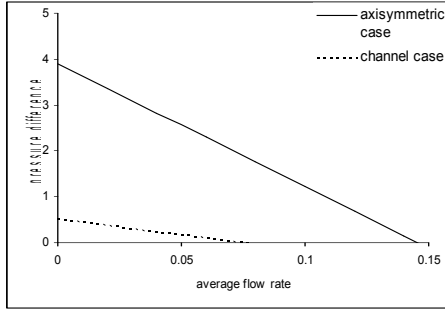


Figure 3: Pressure vs. average flow rate. Dotted line (.....) represents the said relation for channel flow and continuous line (—) represents the same relation for axisymmetric flow for  $\phi = 0.2$ .

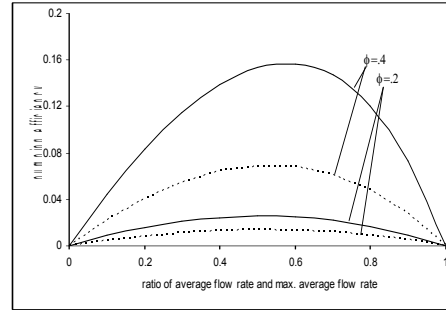


Figure 4: Mechanical efficiency vs. ratio of average flow rate and maximum average flow rate. Dotted lines (.....) represent efficiency of peristaltic pump for different amplitudes in channel flow and continuous lines (—) represent efficiency of peristaltic pump for different amplitude in axisymmetric flow.

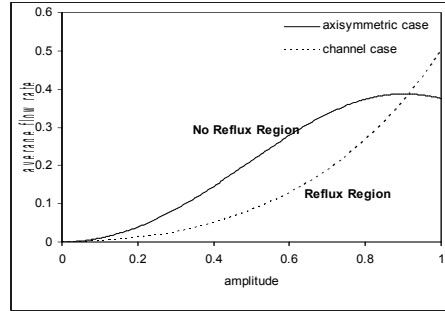


Figure 5: Average flow rate vs. amplitude. The dotted line (.....) represents reflux limit for finite length vessels in channel flow and continuous line (—) represents reflux limit for finite length vessels in axisymmetric flow.

### 5.3 Reflux

Reflux is the other phenomenon that we study here for the present case under the influence of unidirectionally vibrating walls. A graph is plotted for  $\phi$  vs.  $\bar{Q}$  based on Eq.4.10 for planer case and Eq.4.19 for tubular case, to study the reflux limit. Fig.5 reveals that the higher the amplitude of the wave, the higher is the averaged flow rate for reflux to take place. This is depicted by the dotted line for channeling and continuous line for tubular vessel. It is found that limiting curve constantly rises in the channel case while in the tubular case, the curve rises initially but once it attains a particular height it tends to yield. There is a point, say yield point, where the two curves intersect each other, revealing a common value of flow rate for a particular value of amplitude which is very high in magnitude. A further decline of the curve till it meets the situation of total occlusion, discloses that in this case, reflux can take place at a lower flow rate if the tube undergoes higher occlusions. Another important revelation is that reflux will occur at comparatively higher flow rate until the yield point is reached if the flow is tubular. However, at very high occlusions, i.e., beyond the yield point the comparative results are reversed.

## 6 Conclusion

Computer simulation of the model reveals that pressure distribution for channel flow along the length of a vessel of finite size is similar to that for tubular flow although there is a significant difference in the distribution pattern if the wall motion is changed even a bit. Thus, this is inferred that the exact pattern of pressure distribution for the oesophagus can be had only if the real and exact wall equation is known. It is further observed during temporal examination that local wall shear stress distributions for channel and tubular flows are qualitatively similar but quantitatively quite different.

An investigation of mechanical efficiency indicates that larger occlusions will make pumping more efficient and that the tubes are better pumps than channels.

Moreover, it is further concluded that when the vessel is less squeezed, planar flow is more likely to reverse the flow whereas when occlusion of the vessel is nearly total, tubular flow is more prone to the occurrence of reflux.

## References

- [1] Shapiro A. H., Jaffrin M.Y., and Weinberg S. L., Peristaltic Pumping with Long Wavelengths at Low Reynolds Number, *J. Fluid Mech.*, 35 669-675 (1969).
- [2] Dorst Keri, Esophageal reflux disease, 2 Nutrition Bytes; Article1.
- [3] Takabatake S. and Ayukawa K., Numerical study of two-dimensional peristaltic flows, *J. Fluid Mech.*, 122 439-465 (1982).
- [4] Takabatake S., Ayukawa K. and Mori A., Peristaltic pumping in circular cylindrical tubes: a numerical study of fluid transport and its efficiency, *J. Fluid Mech.*, 193 267-283 (1988).
- [5] Brasseur J. G., Corrsin S. and Lu N. Q., The influence of a peripheral layer of different viscosity on peristaltic pumping with Newtonian fluids, *J. Fluid Mech.*, 174 495-519 (1987).
- [6] Rao A. R. and Usha S., Peristaltic transport of two immiscible viscous fluids in a circular tube, *J. Fluid Mech.*, 298 271-285 (1995).
- [7] Usha S. and Rao A. R., Peristaltic Transport of a bio-fluid in a pipe of elliptic Cross section, *J. Biomechanics*, 28 45-52 (1995).
- [8] Misra J. C. and Pandey S. K., Peristaltic transport of a non-Newtonian fluid with a peripheral layer, *Int. J. country-regionplaceEng. Sci.*, 37 1841-1858 (1999).
- [9] Misra J. C. and Pandey S. K., Peristaltic flow of a multilayered power-law fluid through a cylindrical tube, *Int. J.Eng. Sci.*, 39 387-402 (2001).
- [10] Eytan Osnat, Jaffa A. J. and Elad David, Peristaltic flows of a tapered channel: application to embryo transport within the uterine cavity, *Medical Engineering & Physics*, 23 473-482 (2001).
- [11] Elshehawey E. F. and Gharsseldien Z. M., Peristaltic transport of three layered flow with variable viscosity, *Applied mathematics and computation*, 153 417-432 (2004).
- [12] Rao A. R. and Mishra M., Peristaltic transport of a power-law fluid in a porous tube, *J. Non-Newtonian Fluid Mech.*, 121 163-174 (2004).
- [13] Rao A. R. and Mishra M., Peristaltic transport in a channel with a porous peripheral layer: Model of a flow in gastrointestinal tract, *Journal of Biomech.*, 38 779-789 (2005).
- [14] Li Meijing, and Brasseur J. G., Nonsteady Peristaltic Transport Infinite Length Tubes, *J. Fluid Mech.*, 248 129-151 (1993).
- [15] Misra J. C. and Pandey S. K., A Mathematical Model for Oesophageal Swallowing of a Food Bolus, *Mathematical and Computer Modelling*, 33 997-1009 (2001).